

1 **Title:** A Single Dose of Self-Transcribing and Replicating RNA Based SARS-CoV-2
2 Vaccine Produces Protective Adaptive Immunity In Mice.

3

4 Authors:

5 Ruklanthi de Alwis^{1,2*}, Esther S Gan^{2*}, Shiwei Chen², Yan Shan Leong¹, Hwee Cheng Tan²,
6 Summer L Zhang², Clement Yau², Daiki Matsuda³, Elizabeth Allen³, Paula Hartman³, Jenny
7 Park³, Maher Alayyoubi³, Hari Bhaskaran, Adrian Dukanovic, Belle Bao³, Brenda
8 Clemente³, Jerel Vega³, Scott Roberts³, Jose A. Gonzalez³, Marciano Sablad³, Rodrigo
9 Yelin³, Wendy Taylor³, Kiyoshi Tachikawa³, Suezanne Parker³, Priya Karmali³, Jared
10 Davis³, Sean M. Sullivan³, Steve G. Hughes³, Pad Chivukula³, Eng Eong Ooi^{1,2}

11

12

13 ¹Viral Research and Experimental Medicine Center, SingHealth Duke-NUS Academic
14 Medical Center, Singapore.

15 ²Program in Emerging Infectious Diseases, Duke-NUS Medical School, Singapore.

16 ³Arcturus Therapeutics, Inc., 10628 Science Center Drive, San Diego CA 92121

17

18 *Equal contribution

19 Correspondence to: Dr. Eng Eong Ooi; engeong.ooi@duke-nus.edu.sg

20

21

22

23

24 Key words

25 SARS-CoV-2, conventional mRNA, self-amplifying RNA, STARR®, LUNAR®-COV19,
26 COVID-19, Vaccine, Coronavirus

27

28

29

30

31

32

33

34

35 **ABSTRACT**

36 A self-transcribing and replicating RNA (STARRTM) based vaccine (LUNAR[®]-COV19) has
37 been developed to prevent SARS-CoV-2 infection. The vaccine encodes an alphavirus-based
38 replicon and the SARS-CoV-2 full length spike glycoprotein. Translation of the replicon
39 produces a replicase complex that amplifies and prolong SARS-CoV-2 spike glycoprotein
40 expression. A single prime vaccination in mice led to robust antibody responses, with
41 neutralizing antibody titers increasing up to day 60. Activation of cell mediated immunity
42 produced a strong viral antigen specific CD8⁺ T lymphocyte response. Assaying for
43 intracellular cytokine staining for IFN- γ and IL-4 positive CD4⁺ T helper lymphocytes as
44 well as anti-spike glycoprotein IgG2a/IgG1 ratios supported a strong Th1 dominant immune
45 response. Finally, single LUNAR-COV19 vaccination at both 2 μ g and 10 μ g doses
46 completely protected human ACE2 transgenic mice from both mortality and even measurable
47 infection following wild-type SARS-CoV-2 challenge. Our findings collectively suggest the
48 potential of Lunar-COV19 as a single dose vaccine.

49

50

51 INTRODUCTION

52 The pandemic of coronavirus disease-2019 (COVID-19) has afflicted tens of millions of
53 people, of which hundreds of thousands have died from severe respiratory dysfunction and
54 other complications of this disease [1]. The etiological agent of COVID-19 is the severe acute
55 respiratory syndrome coronavirus 2 (SARS-CoV-2), which may have first emerged from a
56 zoonotic source to then spread from person-to-person until global dissemination [1]. Current
57 control measures to curb the pandemic, such as national lockdowns, closure of work places
58 and schools and reduction of international travel are threatening to draw the world into a
59 global economic recession of unprecedented scale [2]. Vaccines that elicit durable protection
60 against SARS-CoV-2 infection are thus urgently needed [3]. Encouragingly, hundreds of
61 different vaccine development efforts are currently in progress, some of which have even
62 entered phase III clinical trials [4, 5].

63

64 Despite some candidates reaching late-stage clinical trials, there is some uncertainty that
65 production can be upscaled in a sufficiently accelerated timeline to manufacture the billions
66 of vaccine doses required to immunize the world's population [6]. Furthermore, recent results
67 from early phase COVID-19 vaccine trials have suggested that more than one dose would be
68 needed to elicit reasonable levels of adaptive immune memory [7-9]. Durable protection with
69 a single dose has been achieved with some viral live-attenuated vaccines (LAV), such as the
70 yellow fever vaccine [10-12]. However, since the genetic determinants of the clinical fitness
71 of SARS-CoV-2 are not well defined, development of a LAV SARS-CoV-2 strain that is safe
72 for use in humans is challenging. An alternative approach would be to mimic the key
73 immunogenic properties of live viral vaccines, to develop an alternate vaccine platform that
74 could also be effective in preventing COVID-19 with a single dose. A single dose vaccine
75 would not only avoid logistics and compliance challenges associated with multi-dose
76 vaccines, but also allow vaccination of more individuals with each batch [6].

77

78 RNA vaccines offer a rapid approach to develop a COVID-19 vaccine [13]. RNA vaccines
79 are designed using the genetic sequence of the viral antigen and rapidly manufactured using
80 cell-free, rapidly scalable techniques [14]. The RNA is encapsulated in a lipid nanoparticle
81 (LNP), which generates robust immune responses without the need for adjuvants [15, 16].
82 There are two main categories of RNA vaccines; 1) the conventional messenger RNA
83 (conventional mRNA) vaccine, where the immunogen of interest is directly translated from
84 the input vaccine transcript, and 2) the newer self-replicating RNA (replicon) vaccines [14].

85 Replicon vaccines encode replication machinery, usually alphavirus-based replication
86 complex, that amplify sub-genomic RNA carrying the antigen of interest, resulting in the
87 amplification of transcripts bearing the antigen by several orders of magnitude over the initial
88 dose [17]. Prolonged antigen expression by such a construct could not only produce the
89 obvious dose sparing effects [17] but potentially also elicit innate and adaptive immune
90 responses similar to those associated with live vaccines. Herein, we show a head-to-head
91 comparison between a self-replicating RNA vaccine using Arcturus' proprietary Self-
92 Transcribing and Replicating RNA (STARRTM technology and a conventional mRNA
93 vaccine against SARS-CoV-2 and suggest that the STARR vaccine, LUNAR-COV19 offers
94 superior vaccine-induced immune responses to conventional mRNA.

95

96 **RESULTS**

97

98 ***Comparison of design and expression of STARR and conventional mRNA platforms***

99 Both LUNAR-COV19 and conventional mRNA vaccine constructs were designed to encode
100 the full-length, unmodified, pre-fusion SARS-CoV-2 S protein (1273 aa), with LUNAR-
101 COV19 additionally encoding the Venezuelan equine encephalitis virus (VEEV) replicase
102 genes required for self-amplification (**Figure 1A**). We first defined the characteristics of
103 these different constructs, which were both formulated with the same LUNAR LNP lipid
104 formulation. Despite differences in RNA lengths for LUNAR-COV19 and conventional
105 mRNA, the LNP diameter, polydispersity index and RNA trapping efficiency were similar
106 (**Figure 1B**). *In vitro* expression of the LUNAR-COV19 and conventional mRNA vaccine
107 were confirmed in cell lysate 24 hours post-transfection through positive western blot
108 detection of the S protein (**Figure 1C**). It was also observed that both vaccines expressed a
109 mixture of full-length S protein and cleaved S protein, i.e. into S1 and S2 transmembrane and
110 cytoplasmic membrane domains (**Figure 1C**). We then compared *in vivo* protein expression
111 of the two RNA platforms in BALB/c mice, by using STARR and conventional mRNA
112 constructs that expressed a luciferase reporter (**Figure 1D**). As expected, animals injected
113 with the conventional mRNA vaccine construct showed high *in vivo* luciferase expression at
114 day 1 although the expression levels declined significantly three days post injection. In
115 contrast, the luciferase expression in STARR injected mice showed increased signal of
116 protein production compared to conventional mRNA at all time points after Day 1 up to Day
117 7 post-inoculation (the last time point measured) and at doses ≥ 2.0 μg , protein expression

118 appeared to be still rising at day 7 (**Figure 1D**). These data showed that dose-for-dose, the
119 STARR luciferase construct yielded higher and more prolonged duration of luciferase
120 expression compared to mice injected with the conventional mRNA luciferase construct.

121

122 *Immune gene expression following LUNAR-COV19 and conventional mRNA vaccination*

123 C57BL/6J mice were vaccinated with LUNAR-COV19 or conventional mRNA vaccines at
124 0.2 µg, 2 µg and 10 µg doses or PBS control. No significant mean loss in animal weight
125 occurred over the first 4 days, except for those that received 10 µg of LUNAR-COV19
126 (**Figure 2A**). However, apart from weight loss, there were few other clinical signs as
127 indicated by the minimal differences in clinical scores. Both weight and clinical scores
128 improved uneventfully after day 3 post vaccination.

129

130 The innate immune response, particularly the type-I interferon (IFN) response has previously
131 been shown to be associated with vaccine immunogenicity following yellow fever
132 vaccination [11, 12, 18]. Furthermore, we have also found that reactive oxygen species-
133 driven pro-inflammatory responses underpinned systemic adverse events in yellow fever
134 vaccination [19, 20]. Therefore, we measured the expression of innate immune and pro-
135 inflammatory genes in whole blood of C57BL/6 mice inoculated with either PBS,
136 conventional mRNA vaccine or LUNAR-COV19. Genes in the type-I IFN pathway were the
137 most highly expressed in animals inoculated with LUNAR-COV19 compared to either
138 conventional mRNA vaccine or PBS (**Figure 2B** and **Supplementary Figure 1**). By contrast,
139 genes associated with pro-inflammatory responses were mostly reduced in abundance
140 following LUNAR-COV19 vaccination compared with either conventional mRNA vaccine or
141 PBS (**Figure 2B** and **Supplementary Figure 1**).

142

143 Since adaptive immune responses develop in germinal centers in the draining lymph nodes,
144 we dissected the draining lymph nodes at day 7 post-inoculation (study schematic in **Figure**
145 **2A**). The inguinal lymph nodes of mice inoculated with LUNAR-COV19 showed a dose-
146 dependent increase in weight, unlike those from mice inoculated with either conventional
147 mRNA vaccine or PBS; the mean weight of lymph nodes from mice given 10 µg of LUNAR-
148 COV19 was significantly higher than those given the equivalent conventional mRNA vaccine
149 (**Figure 2C**). Principal component analysis (PCA) of immune gene expression showed
150 clustering of responses to each of the 3 doses of LUNAR-COV19 away from the PBS control

151 (depicted as red and orange spheres in **Figure 2D-F**), indicating clear differences in immune
152 gene expression between LUNAR-COV19 vaccinated and placebo groups. These trends were
153 also dissimilar to those from mice given conventional mRNA vaccine where at all tested
154 doses, the PCA displayed substantial overlap with PBS control (shown as blue and orange
155 spheres in **Figure 2D-F**).

156

157 We next assessed the differentially expressed genes in the lymph nodes of mice given
158 LUNAR-COV19 compared to those inoculated with mRNA vaccine. Volcano plot analysis
159 identified significant upregulation of several innate, B and T cells genes in LUNAR-COV19
160 immunized animals (**Figure 2G-I**). Some of the most highly differentially expressed genes
161 included, GZMB (required for target cell killing by cytotoxic immune cells) [21], S100A8
162 and S100A9 (factors that regulate immune responses via TLR4) [22], TNFRSF17 (also
163 known as BCMA and regulates humoral immunity) [23], CXCR3 (chemokine receptor
164 involved in T cell trafficking and function) [24] and AICDA (mediates antibody class
165 switching and somatic hypermutation in B cells) [25]. These findings collectively indicate
166 that the adaptive immune responses in the draining lymph nodes of mice inoculated with
167 LUNAR-COV19 may differ to those given the non-replicating mRNA vaccine.

168

169 *LUNAR-COV19 induced robust T cell responses*

170 We next investigated the cellular immune response following vaccination of C57BL/6 mice
171 ($n=5$ per group) with LUNAR-COV19 or conventional mRNA. At day 7 post-vaccination,
172 spleens were harvested and assessed for CD8 and CD4 T cells by flow-cytometry. The CD8+
173 T cell CD44+CD62L- effector/memory subset was significantly expanded in LUNAR-
174 COV19 vaccinated mice compared to those given either PBS or conventional mRNA vaccine
175 (**Figure 3A-B**). There was no statistically significant difference in the proportion of CD4+ T
176 effector cells in these animals (**Figure 3C**). IFN γ + CD8+ T cells (with 2 μ g and 10 μ g doses)
177 and IFN γ + CD4+ T cells (in 0.2 μ g and 10 μ g) were proportionately higher, as found using
178 intracellular staining (ICS) with flow cytometry, in LUNAR-COV19 as compared to
179 conventional mRNA vaccinated animals (**Figure 3D-F**).

180

181 SARS-CoV-2 specific cellular responses were assessed in vaccinated animals by ELISPOT.
182 A set of 15-mer peptides covering the full length SARS-CoV-2 S protein were divided into 4
183 pools and tested for IFN γ + responses in splenocytes of vaccinated and non-vaccinated

184 animals. SARS-CoV-2-specific cellular responses (displayed as IFN γ ⁺ SFU/10⁶ cells) were
185 detected by ELISPOT in both LUNAR-COV19 and conventional mRNA vaccine immunized
186 animals compared to PBS control (**Figure 3G-I**). These responses were substantially higher
187 across all doses in LUNAR-COV19 compared to conventional mRNA vaccinated groups
188 (**Figure 3G-I**). Even the highest tested dose (10 μ g) of conventional mRNA vaccine
189 produced IFN γ ⁺ ELISPOT responses that were appreciably lower than those by the lowest
190 dose (0.2 μ g) of LUNAR-COV19.

191

192 *LUNAR-COV19 induced superior humoral immune responses*

193 SARS-CoV-2-specific humoral responses following vaccination with a single injection were
194 characterized in two different mouse models, BALB/c and C57BL/6. Female mice ($n=5$ per
195 group) were vaccinated at day 0 and bled every 10 days, up to day 60 for BALB/c and day 30
196 for C57BL/6 (**Figure 4A**). SARS-CoV-2 S-specific IgM responses were tested at 1:2000
197 serum dilution using an in-house Luminex immuno-assay. All tested doses of the
198 conventional mRNA vaccine and LUNAR-COV19 produced detectable S-specific IgM
199 responses in both mouse models (**Figure 4B-C**). When comparing LUNAR-COV19 to
200 conventional mRNA vaccinated BALB/c mice, no difference in IgM responses was observed;
201 IgM levels in C57BL/6 mice were higher in LUNAR-COV19 vaccinated C57BL/6 mice at
202 day 10 post vaccination. In contrast, SARS-CoV-2 S-specific IgG (at 1:2000 serum dilution)
203 levels were universally higher from day 20 onwards in animals inoculated with LUNAR-
204 COV19 compared to conventional mRNA vaccine (**Figure 4D-E**). Perhaps even more
205 remarkably, in BALB/c vaccinated with LUNAR-COV19, the IgG levels continued to
206 increase until day 50 post-vaccination; C57BL/6 mice were only monitored until day 30 post-
207 vaccination. This trend contrasted sharply with mice that received the conventional mRNA
208 vaccine where in BALB/c mice antibody levels plateaued after day 10 post-vaccination;
209 although increasing S-specific IgG levels were observed in conventional mRNA-vaccinated
210 C57BL/6 mice these were universally lower than those that received LUNAR-COV19.

211

212 In depth characterization of the SARS-CoV-2 specific IgG response in vaccinated animals
213 was conducted at day 30 post-immunization to assess which regions of S protein are targeted.
214 IgG endpoint titers were estimated to full ectodomain S protein, S1, S2 and receptor binding
215 domain (RBD) regions. As expected for both vaccine candidates the majority of SARS-CoV-
216 2 specific IgG recognized S1, which contains the RBC, although high IgG endpoint titers

217 were also detected to S2 protein (**Figure 4F-G**). However, LUNAR-COV19 elicited IgG
218 endpoint titers were universally and significantly higher compared to those produced by
219 conventional mRNA vaccination (**Figure 4F-G**). Notably, IgG that bind the RBD of S
220 protein, which is an immunodominant site of neutralizing antibodies [26, 27], were also
221 higher in LUNAR-COV19 compared to conventional mRNA vaccinated animals. It is also
222 noteworthy that at lower doses, conventional mRNA vaccine but not LUNAR-COV19
223 struggled to elicit high SARS-CoV-2 specific IgG titers in the more Th1 dominant C57BL/6
224 mouse strain (**Figure 4G**). Taken collectively, a single dose of LUNAR-COV19 induced
225 significant differences in immune gene expression and superior cellular immune responses in
226 draining lymph nodes compared to the conventional mRNA vaccine and consequently greater
227 and more prolonged humoral immune responses.

228

229 We assessed both the binding strength (avidity) and the neutralizing ability of the antibody
230 response elicited by these vaccine constructs. Serum IgG avidity was measured at day 30
231 post-vaccination using a modified Luminex immuno-assay with 8M urea washes. LUNAR-
232 COV19 elicited higher avidity S protein-specific IgG in both mouse models at all tested
233 doses (**Figure 4H**). These differences were observed, with the exception of 0.2 μ g in
234 BALB/c, across all doses (**Figure 4H**), indicating that LUNAR-COV19 elicited better quality
235 antibodies, suggesting superior affinity maturation with the LUNAR-COV19 vaccine.

236

237 Neutralization of live SARS-CoV-2 by serum from vaccinated animals was assessed using
238 the plaque reduction neutralization test (PRNT). At day 30 LUNAR-COV19 vaccinated
239 BALB/c mice showed a clear dose-dependent elevation in PRNT₅₀ titers; 4 out of 5 (80%) of
240 mice in the 10 μ g LUNAR-COV19 group showed PRNT₅₀ titers greater than 320, which was
241 the upper limit of our dilution (**Figure 4I**). Similar dose-dependent trends in PRNT₅₀ titers
242 were also found in C57BL/6 mice although in these animals, the PRNT₅₀ titers of several
243 animals exceeded 320 even with the lowest 0.2 μ g dose vaccination (**Figure 4I**). In sharp
244 contrast, PRNT₅₀ titers in animals inoculated with the conventional mRNA vaccine construct
245 were, except for one C57BL/6J mouse that received 10 μ g dose, all <20 (**Figure 4I**).

246 Unexpectedly but encouragingly, PRNT₅₀ and PRNT₇₀ titers of LUNAR-COV19 vaccinated
247 BALB/c mice continued to rise between day 30 and day 60 after a single vaccination (**Figure**
248 **4J-K**) and at both time points for doses ≥ 2.0 μ g. These titers were comparable to PRNT₇₀
249 titers for sera from convalescent COVID-19 patients (**Figure 4K**).

250

251 We also found that the S protein IgG titers positively correlated with PRNT₅₀ titers with
252 LUNAR-COV19 vaccinated mice in both mouse models (**Figure 4L**). Similar positive
253 correlations were also observed with IgG against S1 and RBD (**Supplementary Figure 1**).
254 By contrast, we found no correlation between IgG and PRNT₅₀ titers in conventional mRNA
255 vaccinated mice (**Figure 4L**). Taken collectively, our antibody response analyses suggest that
256 the higher PRNT₅₀ titers following vaccination with LUNAR-COV19 are not only strongly
257 associated with the amount of IgG produced but are also a factor of the superior quality of the
258 anti-SARS-CoV-2 antibodies produced following vaccination with LUNAR-COV19.

259

260 *LUNAR-COV19 vaccination showed a Th1 dominant response*

261 A safety concern for a coronavirus vaccine is the risk of vaccine-associated immune
262 enhancement of respiratory disease (VAERD) [28]. Indeed, SARS-CoV and MERS-CoV
263 vaccine development have highlighted the importance of Th1 skewed responses in mitigating
264 the risk of vaccine-induced immune enhancement [29, 30]. Therefore, we investigated the
265 Th1/ Th2 balance elicited by vaccination with both conventional mRNA and LUNAR-
266 COV19. The IgG subclass fate of plasma cells are highly influenced by T helper (Th) cells
267 [31]. At day 30 post-vaccination, both conventional mRNA and LUNAR-COV19, induced
268 comparable amounts of SARS-CoV-2 S-specific IgG1, a Th2-associated IgG subclass in
269 mice, except for the 0.2 µg dose in C56BL/6J mice (**Figure 5A-B**). In contrast, the Th1-
270 associated IgG subclasses - IgG2a in BALB/c and IgG2c in C56BL/6J - were significantly
271 greater in LUNAR-COV19 vaccinated animals. The ratios of S protein-specific IgG2a/IgG1
272 (Balb/c) and IgG2c/IgG1 (C57BL/6) were greater than 1 in LUNAR-COV19 vaccinated
273 animals (**Figure 5A-B**). Except for the 0.2 µg dose, these ratios were all significantly greater
274 with LUNAR-COV19 compared to the conventional mRNA vaccinated animals.

275

276 Additionally, we used ICS to investigate the production of IFN γ (Th1 cytokine) and IL4 (Th2
277 cytokine) by CD4⁺ T cells in spleens at day 7 post vaccination C56BL/6J mice. As was
278 described above, compared to conventional mRNA vaccination, IFN γ levels were
279 significantly greater in LUNAR-COV19 vaccinated animals (Figure 3F). IL4 expression in
280 CD4 T cells were slightly higher with conventional mRNA as compared to LUNAR-COV19
281 at 0.2 and 2.0 µg doses (**Figure 5C**). In comparing the IFN γ and IL4 levels in individual
282 mice, we found that the ratios of IFN γ /IL4 in CD4⁺ T cells for both LUNAR-COV19 and

283 conventional mRNA vaccinated mice were universally above 1 (**Figure 5D**). The ratio of
284 IFN γ /IL4 in CD4⁺ T cells in mice given the 0.2 and 2.0 μ g doses were significantly greater
285 with LUNAR-COV19 than conventional mRNA vaccination (**Figure 5F**). However, the
286 elevated ratios at these doses were due to a decrease in IL4 expression at levels below
287 background (i.e. PBS control mice), rather than reduced IFN γ and hence Th1 activity. Taken
288 collectively, our data show that LUNAR-COV19 produced a Th1 biased adaptive immune
289 response.

290

291 *Single dose of LUNAR-COV19 protects from a lethal infection of SARS-CoV-2*

292 Finally, we tested the efficacy of LUNAR-COV19 in protecting against infection and
293 mortality in a lethal SARS-CoV-2 challenge model. Transgenic hACE2 mice immunized
294 with either PBS, or 2 μ g or 10 μ g of LUNAR-COV19 vaccine were intranasally challenged
295 with live SARS-CoV-2 virus (5×10^4 TCID₅₀) at day 30 post-vaccination. This was the same
296 isolate as that used for our PRNT assays. Mice were then divided into two groups: one group
297 was tracked for weight, clinical scores and survival; a second group of mice were euthanized
298 at 5 days post injection (dpi) and viral loads assessed in the respiratory tract (trachea to lung)
299 and brain (**Figure 6A**). Measurement of PRNT₇₀ titers confirmed the generation of
300 neutralizing antibodies in LUNAR-COV19-vaccinated hACE2 mice (**Figure 6B**).
301 Irrespective of tested dosages, mice that received the LUNAR-COV19 vaccine showed
302 unchanged weight and no clinical sign, while the PBS mice showed significant drop in
303 weight and increased clinical scores upon challenge with wild-type SARS-CoV-2 (**Figure**
304 **6C-D**). LUNAR-COV19 vaccination at both 2 μ g and 10 μ g doses fully protected hACE2
305 mice from an otherwise 100% mortality at day 7 post-challenge (**Figure 6E**). Assessment of
306 tissue viral load at day 5 post-challenge found minimal to no SARS-CoV-2 RNA (**Figure 6F**)
307 in contrast to unvaccinated animal controls. Although viral RNA was detectable at very low
308 levels in some animals, this was not associated with any presence of infectious viral particles,
309 so most likely represents viral RNA fragments rather than intact viral RNA genomes. No
310 detectable infectious virus was found in either the respiratory tracts or brains of LUNAR-
311 COV19 vaccinated animals (**Figure 6G**). By contrast, unvaccinated animals showed 4 and 8
312 logs of infectious SARS-CoV-2 in the respiratory tract and brain, respectively (**Figure 6G**).
313 Collectively, these data show that a single dose of LUNAR-COV19 vaccine induced robust
314 humoral and cellular immune responses that led to complete protection of hACE2 mice from
315 a lethal SARS-CoV-2 challenge.

316

317 **DISCUSSION**

318 The pandemic of COVID-19 has necessitated rapid development of vaccines. Encouragingly,
319 several COVID-19 vaccine candidates are now in clinical trials and more are entering first-in-
320 human trials. However, the majority of vaccine candidates being developed require two or
321 more doses for sufficient adaptive immune responses. Requirement for a second shot could
322 complicate compliance rate in mass vaccination campaigns and results in fewer subjects
323 vaccinated per batch, thereby reducing the efficiency of vaccination. Hence, a single dose
324 vaccine that generates robust and sustained cellular and humoral immunity, without elevating
325 the risk of vaccine-mediated immune enhancement, remains an unmet need.

326

327 Amongst the licensed vaccines for other diseases, live attenuated vaccines can offer the most
328 durable protection against viral diseases. Live vaccines infect and replicate at sites of
329 inoculation and some even in draining lymph nodes. Replication enables endogenous and
330 sustained expression of viral antigens that enable antigen presentation to stimulate cytotoxic
331 CD8⁺ T cells. Expressed antigens taken up by antigen presenting cells also trigger CD4⁺ T
332 cell help that drives affinity maturation in B cells. Studies on the live attenuated yellow fever
333 vaccine, have shown that a longer period of stimulation of the adaptive immune response
334 results in superior adaptive immune responses [32]. Although work to determine which of
335 these correlates of live vaccines are mechanistic determinants of adaptive immunity is still
336 ongoing, the ability of self-replicating RNA vaccines to simulate the sustained antigen
337 presentation characteristics of live vaccination could offer durable immunity against COVID-
338 19.

339

340 Numerous studies have shown RNA vaccines to be immunogenic. In this study, we
341 conducted a side-by-side comparison of the immunogenicity elicited by two SARS-CoV-2
342 RNA vaccine candidates, a conventional mRNA construct and the STARR construct,
343 LUNAR-COV19. We found that, compared to conventional mRNA, LUNAR-COV19
344 produced higher and longer protein expression *in vivo*, upregulated the gene expression of
345 several innate, B and T cell response genes in the blood and draining lymph nodes. These
346 properties were associated with significantly greater neutralizing antibody and SARS-CoV-2
347 specific IgG responses, CD8⁺ T cell responses, IFN γ ⁺ ELISPOT responses, and Th1 skewed
348 responses (which have been shown to associate with protection from VAERD) than

349 conventional mRNA. Interestingly, despite the highest tested dose of conventional mRNA
350 eliciting comparable S protein-specific antibodies as the lowest tested dose of LUNAR-
351 COV19, the conventional mRNA-elicited IgG did not show such robust avidity or
352 neutralization activity as those from LUNAR-COV19 vaccination. These data suggest a
353 qualitatively better humoral immune response with superior affinity maturation of B-cells
354 with the LUNAR-COV19 vaccine. Our findings thus highlight the immunological advantages
355 of self-replicating RNA over conventional mRNA platforms.

356

357 The superior quality of immune responses elicited by LUNAR-COV19 over the conventional
358 mRNA vaccine construct could be attributable to multiple factors. Higher and longer
359 expression of immunogens produce better immunity [32], likely through better engagement
360 of T follicular helper cells and thereby leading to more diverse antibody targets and more
361 robust neutralizing antibody responses [33, 34]. Replication of LUNAR-COV19 results in the
362 formation of a negative-strand template for production of more positive-strand mRNA and
363 sub-genomic mRNA expressing the S transgene. Interaction between the negative- and
364 positive-strands forms a double stranded RNA (dsRNA) intermediate, which would interact
365 with TLR3 and RIG-I-like receptors to stimulate type 1 interferon responses [35-37], which
366 we and others have previously shown to correlate with superior adaptive immune responses
367 [11, 12, 18]. Production of IFN γ can also stimulate development of cytotoxic CD8⁺ T cells
368 [36]. Importantly, the S protein does contain human CD8⁺ T cell epitopes. As suggested by
369 recent findings on T cell responses to SARS-CoV-2 and other coronavirus infections [38-40],
370 the development of T cell memory could be important for long-term immunity.

371

372 It is unclear whether the VEEV nsP1-4 forming the replication complex contains any
373 immunogenic properties although mutations in the nsP proteins have been shown to affect the
374 induction of type I IFN [41]. Although unexplored in our current study, VEEV replicons have
375 also been shown to adjuvant immune responses at mucosal sites [42], further justifying the
376 use of STARR platform to develop a COVID-19 vaccine.

377

378 In conclusion, STARR vaccine platform as exemplified by LUNAR-COV19, offers an
379 approach to simulate key immunogenic properties of live virus vaccination and offers the
380 potential for an effective single-shot vaccination against COVID-19.

381

382 **METHODS (Supplement 1)**

383 *Vaccine plasmid constructs and design*

384 A human codon-optimized spike (S) glycoprotein gene of SARS-CoV-2 (GenBank
385 accession: YP_009724390) was cloned into plasmids pARM2922 and pARM2379 for
386 generation of SARS-CoV-2 Spike expressing STARR and conventional mRNA, respectively.
387 The STARR plasmid also encoded for the Venezuela equine encephalitis virus (VEEV) non-
388 structural proteins nsP1, nsP2, nsP3 and nsP4, which together form the replicase complex that
389 bind to the sub-genomic promoter placed right before the S protein sequence. The cloned
390 portions of all plasmid constructs were verified by DNA sequencing. Plasmids were
391 linearized immediately after the poly(A) stretch and used as a template for *in vitro*
392 transcription reaction with T7 RNA polymerase. For LUNAR-CoV19 vaccine, the reaction
393 for RNA was performed as previously described [43] with proprietary modifications to allow
394 highly efficient co-transcriptional incorporation of a proprietary Cap1 analogue and to
395 achieve high quality RNA molecule of over 11,000-nt long the STARR mRNA. RNA was
396 then purified through silica column (Macherey Nagel) and quantified by UV absorbance. For
397 the conventional mRNA vaccine, the RNA was synthesized similarly but with 100%
398 substitution of UTP with N1-methyl-pseudoUTP. For both LUNAR-CoV19 and
399 conventional mRNA vaccines, the RNA quality and integrity were verified by 0.8-1.2% non-
400 denaturing agarose gel electrophoresis as well as Fragment Analyzer (Advanced
401 Analytical). The purified RNAs were stored in RNase-free water at -80 °C until further use.

402

403 *Vaccine lipid nanoparticles (LNPs)*

404 LUNAR® nanoparticles encapsulating STARR™ were prepared by mixing an ethanolic
405 solution of lipids with an aqueous solution of STARR™ RNA. Lipid excipients (Arcturus
406 Therapeutics proprietary ionizable lipid, DSPC, Cholesterol and PEG2000-DMG) are
407 dissolved in ethanol at mole ratio of 50:10: 38.5:1.5 or 50:13:35.5:1.5. An aqueous solution
408 of the vaccine RNA is prepared in citrate buffer pH 4.0. The lipid mixture is then combined
409 with the vaccine RNA solution at a flow rate ratio of 1:3 (V/V) via a proprietary mixing
410 module. Nanoparticles thus formed are stabilized by dilution with phosphate buffer followed
411 by HEPES buffer, pH 8.0. Ultrafiltration and diafiltration (UF/DF) of the nanoparticle
412 formulation is then performed by tangential flow filtration (TFF) using modified PES hollow-
413 fiber membranes (100 kDa MWCO) and HEPES pH 8.0 buffer. Post UF/DF, the formulation
414 is filtered through a 0.2 µm PES filter. An in-process RNA concentration analysis is then

415 performed. Concentration of the formulation is adjusted to the final target RNA concentration
416 followed by filtration through a 0.2 µm PES sterilizing-grade filter. Post sterile filtration,
417 bulk formulation is aseptically filled into glass vials, stoppered, capped, and frozen at $-70 \pm$
418 10°C . Analytical characterization included measurement of particle size and polydispersity
419 using dynamic light scattering (ZEN3600, Malvern Instruments), pH, Osmolality, RNA
420 content and encapsulation efficiency by a fluorometric assay using Ribogreen RNA reagent,
421 RNA purity by capillary electrophoresis using fragment analyzer (Advanced Analytical),
422 lipid content using HPLC,.

423 *In vitro transfection and immunoblot detection of spike protein*

424 Hep3b cells (seeded in 6-well plates at a density of 7×10^5 cells/well, a day before) were
425 transfected with purified IVTs (2.5 µg conventional mRNA and 2.5 µg STARR) by
426 Lipofectamine MessengerMax transfection reagent (Thermo Fisher Scientific) according to
427 the manufacturer's instruction. The cells were harvested the next day with a hypotonic buffer
428 (10 mM Tris-HCl, 10 mM NaCl supplemented with protease inhibitor cocktail (Roche))
429 followed by sonication. Samples were deglycosylated followed by treatment with PNGase F
430 (New England Biolabs) according to the manufacture's instruction.

431 The protein lysate (10 µg) was resolved on a 7.5% NuPAGE Tris-Acetate gel (Thermo Fisher
432 Scientific), and the spike protein expression was analyzed by LI-COR Quantitative Western
433 Blot system using a rabbit antibody detecting S1 (40150-T62-COV2, Sino Biologic) and a
434 mouse antibody for S2 region (GTX632604, GeneTex) along with appropriate secondary
435 antibodies (goat anti-rabbit 800 and goat anti-mouse 680).

436 *Animal studies*

437 *BALB/c studies*

438 All BALB/c mouse studies were approved by the Explora Biolabs IACUC and performed
439 under the Animal Care and Use Protocol number EB-17-004-003. A head-to-head
440 comparison of the protein expression of the conventional mRNA and STARR vaccine
441 platforms was conducted using conventional mRNA and STARR constructs expressing a
442 luciferase reporter gene. BALB/c mice (Jackson Laboratory) were intramuscularly (IM) in
443 the *rectus femoris* with conventional mRNA or STARR at doses of 0.2, 2 and 10 µg ($n=3$
444 mice/group). Expression of the conventional mRNA and STARR constructs were measured

445 at days 1, 3 and 7 post-inoculation through luciferase expression by imaging the mice for
446 bioluminescence.

447

448 Humoral responses to the SARS-CoV-2 Spike vaccine candidates were tested in Female
449 BALB/c mice (Jackson Laboratory) aged 8-10 weeks by IM immunization of the *rectus*
450 *femoris* with either conventional mRNA or LUNAR-COV19 at doses 0.2 µg, 2 µg, or 10 µg
451 ($n=5$ mice/group). Mice were bled at baseline and at 10, 19, 30, 40, 50- and 60-days post-
452 vaccination to assess SARS-CoV-2 specific humoral immune responses.

453

454 *C57BL/6*

455 All *C57BL/6* mouse studies were performed in accordance with protocols approved by the
456 Institutional Animal Care and Use Committee at Singapore Health Services, Singapore (ref
457 no.: 2020/SHS/1554). *C57BL/6* mice purchased from inVivos were housed in a BSL-2
458 animal facility at Duke-NUS Medical School. Groups of 6-8 weeks old wild-type *C57BL/6*
459 female mice were vaccinated intramuscularly with either conventional mRNA or LUNAR-
460 COV19 at doses 0.2 µg, 2 µg, or 10 µg. For transcriptomic and T cell studies, submandibular
461 bleeds were performed for whole blood at 24 hrs post-vaccination. Day 7 post-immunization,
462 mice were sacrificed and inguinal lymph nodes and spleen harvested for investigation of
463 immune gene expression and T cell responses, respectively. Splenocyte suspensions for
464 measuring T cell responses were obtained by crushing spleen through a 70µm cell strainer
465 (Corning). Red blood cells were removed by lysis using BD PharmLyse reagent. For
466 antibody studies, another set of vaccinated 6-8 weeks old mice were bled at baseline and at
467 10, 20, and 30 days post-vaccination.

468

469 SARS-CoV-2 challenge experiments were conducted with female B6;SJL-Tg(K18-
470 hACE2)2PrImn/J mice purchased from Jackson laboratory. Groups of 6-8 weeks old wild-
471 type *C57BL/6* female mice were vaccinated intramuscularly with 100 µl LUNAR-COV19 at
472 doses of 2 µg, or 10 µg. Submandibular bleeds were performed for serum isolation to
473 determine antibody titers via PRNT 28 days post vaccination. Animal were infected with
474 5×10^4 TCID₅₀ in 50µl via the intranasal route. Daily weight measurements and clinical
475 scores were obtained. Mice were sacrificed when exhibiting greater than 20% weight loss or
476 clinical score of 10. To assess organ viral loads, mice were sacrificed 5 days post infection
477 and harvested organs were frozen at -80°C. Whole lungs and brains were homogenized with

478 MP lysing matrix A and F according to manufacturer's instructions in 1ml PBS. Homogenate
479 was used to assess both plaque titers and RNA extraction using TRIzol LS (Invitrogen). No
480 blinding was done for animal studies.

481

482 *Gene expression of immune and inflammatory genes*

483 Whole blood collected 1-day post-vaccination was lysed using BD PharmLyse reagent and
484 RNA extracted using Qiagen RNeasy kit. Mouse lymph nodes collected from 7 days post
485 vaccination were homogenized and RNA extracted using trizol LS. RNA (50 ng) from whole
486 blood cells and lymph nodes were hybridized to the NanoString nCounter mouse
487 inflammation and immunology v2 panels (Nanostring Technologies), respectively. As
488 previously described [20, 44], RNA was hybridized with reconstituted CodeSet and
489 ProbeSet. Reactions were incubated for 24 hours at 65°C and ramped down to down to 4°C.
490 Hybridized samples were then immobilized onto a nCounter cartridge and imaged on a
491 nCounter SPRINT (NanoString Technologies). Data was analyzed using the nSolver
492 Analysis software (Nanostring Technologies) and Partek Genomics Suite. For normalization,
493 samples were excluded when percentage field of vision registration is <75, binding density
494 outside the range 0.1–1.8, positive control R^2 value is <0.95 and 0.5 fM positive control is ≤ 2
495 s.d. above the mean of the negative controls. Background subtraction was performed by
496 subtracting estimated background from the geometric means of the raw counts of negative
497 control probes. Probe counts less than the background was floored to a value of 1. The
498 geometric mean of positive controls was used to compute positive control normalization
499 parameters. Samples with normalization factors outside 0.3–3.0 were excluded. The
500 geometric mean of housekeeping genes was used to compute the reference normalization
501 factor. Samples with reference factors outside the 0.10–10.0 range were also excluded.
502 Hierarchical clustering was performed with Partek Genomics Suite v6 on gene sets zScore
503 values by Euclidean dissimilarity and average linkage.

504

505 To identify DEGs between groups, Partek Genomics Suite Analysis v7 software was used to
506 analyse variance (ANOVA) with a cut off-of $P < 0.05$. Log₂ Fold Changes generated were
507 used for volcano plots constructed using Prism v8.1.0 software. DEGs were identified by a
508 fold change cut-off of 2. Unsupervised principle component analysis was performed to
509 visualize variability between vaccinated and non-vaccinated animals with Partek genomics
510 suite analysis v7 software. PCA ellipsoids were drawn with a maximum density and 3
511 subdivisions.

512

513 ***Flow cytometry***

514 Surface staining was performed on freshly-isolated splenocytes using the following panel of
515 antibodies and reagents: B220 (RA3-6B2), CD3 (17A2), CD4 (RM4-5), CD8 α (53-6.7),
516 CD44 (IM7), CD62L (MEL-14) and DAPI. Intracellular cytokine staining was performed by
517 stimulating freshly-isolated splenocytes with 50 ng/ml PMA and 500 ng/ml ionomycin in the
518 presence of GolgiPlug (BD) for 6 h. After stimulation, surface staining of CD3, CD4 and
519 CD8a was performed followed by intracellular staining of IFN- γ (XMG1.2) and IL-4
520 (11B11). Data acquisition was performed on a BD LSRFortessa and analyzed using FlowJo.

521

522 ***ELISPOT***

523 ELISPOT was performed using mouse IFN- γ ELISpot^{BASIC} kit (Mabtech). A similar protocol
524 has been used for human SARS-CoV-2 samples [40]. In brief, 4 x 10⁵ freshly-isolated
525 splenocytes were plated into PVDF-coated 96 well plates containing IFN- γ capture antibody
526 (AN18). Cells were stimulated with a 15-mer peptide library covering part of the S protein.
527 143 total peptides were divided into four pools and used at a final concentration of 1 μ g/ml
528 per peptide. Negative control wells contained no peptide. Following overnight stimulation,
529 plates were washed and sequentially incubated with biotinylated IFN- γ detection antibody
530 (R4-6A2), streptavidin-ALP and finally BCIP/NBT. Plates were imaged using ImmunoSpot
531 analyzer and quantified using ImmunoSpot software.

532

533 ***Luminex Immuno-assay***

534 *Longitudinal assessment of binding antibody*

535 Longitudinal IgM and IgG responses in BALB/c and C57BL/6 were measured using an in-
536 house Luminex Immuno-assay. Similar Luminex Immuno-assays have been previously
537 described for antibody detection against SARS-CoV-2 antigens [45, 46]. Briefly, Magpix
538 Luminex beads were covalently conjugated to insect-derived HIS-tagged SARS-CoV-2
539 whole Spike protein (SinoBiologicals) using the ABC coupling kit (Thermo) as per
540 manufacturer's instructions. Beads were then blocked with 1%BSA, followed by incubation
541 with serum (diluted at 1:2000 in block) for 1 hr at 37C. Beads are then washed and SARS-
542 CoV-2 Spike-specific mouse antibodies were detected using the relevant biotinylated
543 secondary antibody (i.e. anti-mouse IgM-biotin and anti-mouse IgG-biotin (Southern
544 Biotech) for IgM and IgG assessment, respectively) with streptavidin-PE (Southern Biotech).
545 Antibody binding to Spike were then measured on a Magpix instrument as median

546 fluorescence intensity (MFI). Spike antigen quantity on beads were also probed with anti-
547 6xHIS-PE antibodies and all MFI values were then corrected to Spike antigen quantity to
548 account for experiment to experiment variation.

549

550 *IgG and IgG subclass endpoint titers*

551 IgG endpoint titers to mammalian-derived SARS-CoV-2 Spike, Spike domain 1 (S1), spike
552 domain 2 (S2) and receptor binding domain (RBD) at day 30 sera post-immunization were
553 measured using Luminex ImmunoAssay. Assay was conducted as described above, with the
554 modification of serially diluting serum 10-fold from 200 to 2×10^8 . Similarly, IgG subclass
555 endpoint titers (i.e. IgG1 and IgG2a in BALB/c and IgG1 and IgG2c in C57BL/6) were
556 measured against mammalian-derived SARS-CoV-2 Spike protein using serially diluted
557 mouse sera (5-fold from 200 to 3.1×10^6) and secondary antibodies anti-IgG1-biotin, anti-
558 IgG2a-biotin or anti-IgG2b-biotin (Southern Biotech). Four parameter logistic (4PL) curves
559 were fitted to the measured MFI data from serially diluted sera, and three times the
560 background (i.e. 3x MFI with no serum) was used as a threshold cutoff to estimate endpoint
561 titers.

562

563 *IgG Avidity*

564 Avidity index of IgG to SARS-CoV-2 Spike protein at day 30 sera post-immunization was
565 estimated using the Luminex ImmunoAssay. Assay was conducted as described above with
566 the minor modification of following bead incubation with serum (diluted at 1:2000) with
567 either a 10 min PBS or 8M urea wash. Avidity Index was estimated by subtracting
568 background MFI from all sample values, and then dividing MFI with 8M Urea wash by MFI
569 with PBS wash.

570

571 *Neutralization assay*

572 *Virus Neutralization titer assay (VNT)*

573 Neutralization sero-conversion was assessed at day 10 and 20 post-immunization in BALB/c
574 using a virus neutralization assay as previously described [47]. Briefly, sera were diluted to
575 1:20 in culture media, mixed at a 1:1 ratio with a Singaporean clinical isolate of live SARS-
576 CoV-2 virus, isolate BetaCoV/Singapore/2/2020 (GISAID accession code EPI_ISL_406973)
577 and incubated for 1 hr at 37C. Virus-antibody immune-complexes were then added to Vero-
578 E6 cells (ATCC) in 96-well plates, and incubated at 37C. Five days later, plates were
579 assessed under a microscope for cytopathic effect (CPE) of the cells.

580

581 *Plaque reduction neutralization titer (PRNT)*

582 Neutralization of live SARS-CoV-2 was measured by PRNT at day 30 post-vaccination in
583 both BALB/c and C57BL/6 mice. Similar protocols have been published previously for
584 SARS-CoV-2 [48]. Briefly, mouse sera were serially diluted from 1:20 to 1:320 in culture
585 media and incubated with the Singapore isolate of SARS-CoV-2 virus for 1 hr at 37C. Virus-
586 antibody mixtures were then added to Vero-E6 cells in 24-well plates, incubated for 1-2 hrs,
587 then overlaid with carboxymethyl cellulose (CMC) and incubated at 37C under 5% CO₂. At
588 5 days, cells are washed, stained with crystal violet and plaques counted. The serum dilution
589 leading to neutralization of 50% of virus, i.e. PRNT50, was estimated.

590

591 **ACKNOWLEDGMENTS**

592 We thank the Economic Development Board of Singapore for initiating this collaboration and
593 for funding the development of LUNAR-COV19. ARdA received salary support from the
594 National Medical Research Council (NMRC) Young Investigator Award. EEO received
595 salary support from the NMRC Clinician-Scientist Award (Senior Investigator).

596

597 **AUTHOR CONTRIBUTIONS**

598 Ruklanthi de Alwis was responsible for the humoral characterization of the immune response
599 from the LUNAR COV19 vaccine. Esther S Gan was responsible for the huACE2 transgenic
600 mouse challenge studies and expression profiling analysis of the LUNAR COV19 vaccine.

601 **DECLARATION OF INTERESTS**

602 D.M., E.A., P.H., J.P., M.A., H.B., A.D., B.B., B.C., J.V., S.R., J.A.G., M.S., R.Y., W.T.,
603 K.T., S.P., P.K., J.D., S.S., S.H. and P.C. are employees of Arcturus Therapeutics, Inc.

604

605 **REFERENCES**

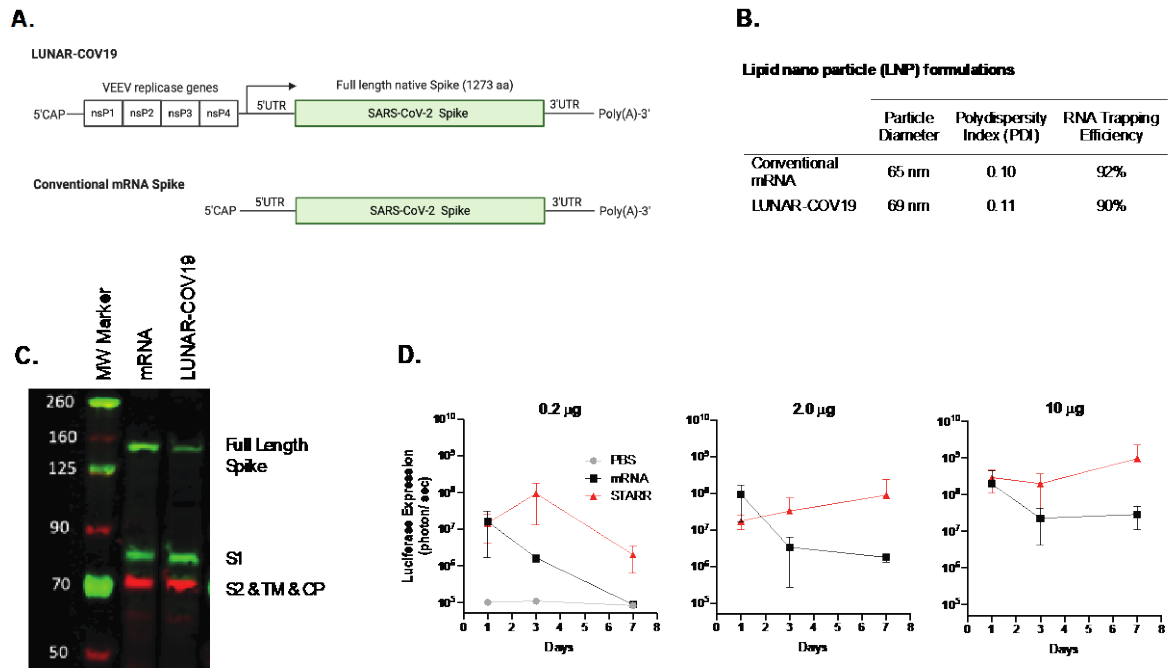
- 606 1. WHO, *WHO Coronavirus Disease (COVID-19) Dashboard*. 2020.
607 2. Bank, W. *The Global Economic Outlook During the COVID-19 Pandemic: A Changed*
608 *World*. 2020; Available from: [https://www.worldbank.org/en/news/feature/2020/06/08/the-](https://www.worldbank.org/en/news/feature/2020/06/08/the-global-economic-outlook-during-the-covid-19-pandemic-a-changed-world)
609 [global-economic-outlook-during-the-covid-19-pandemic-a-changed-world](https://www.worldbank.org/en/news/feature/2020/06/08/the-global-economic-outlook-during-the-covid-19-pandemic-a-changed-world).
610 3. Randolph, H.E. and L.B. Barreiro, *Herd Immunity: Understanding COVID-19*. *Immunity*,
611 2020. **52**(5): p. 737-741.
612 4. WHO. *Draft landscape of COVID-19 candidate vaccines*. 2020; Available from:
613 <https://www.who.int/publications/m/item/draft-landscape-of-covid-19-candidate-vaccines>.
614 5. Thanh Le, T., et al., *The COVID-19 vaccine development landscape*. *Nat Rev Drug Discov*,
615 2020. **19**(5): p. 305-306.
616 6. Lurie, N., et al., *Developing Covid-19 Vaccines at Pandemic Speed*. *N Engl J Med*, 2020.
617 **382**(21): p. 1969-1973.

- 618 7. Folegatti, P.M., et al., *Safety and immunogenicity of the ChAdOx1 nCoV-19 vaccine against*
619 *SARS-CoV-2: a preliminary report of a phase 1/2, single-blind, randomised controlled trial.*
620 *Lancet*, 2020.
- 621 8. Jackson, L.A., et al., *An mRNA Vaccine against SARS-CoV-2 - Preliminary Report.* *N Engl J*
622 *Med*, 2020.
- 623 9. Zhu, F.C., et al., *Safety, tolerability, and immunogenicity of a recombinant adenovirus type-5*
624 *vectored COVID-19 vaccine: a dose-escalation, open-label, non-randomised, first-in-human*
625 *trial.* *Lancet*, 2020. **395**(10240): p. 1845-1854.
- 626 10. Querec, T.D. and B. Pulendran, *Understanding the role of innate immunity in the mechanism*
627 *of action of the live attenuated Yellow Fever Vaccine 17D.* *Adv Exp Med Biol*, 2007. **590**: p.
628 43-53.
- 629 11. Querec, T.D., et al., *Systems biology approach predicts immunogenicity of the yellow fever*
630 *vaccine in humans.* *Nat Immunol*, 2009. **10**(1): p. 116-125.
- 631 12. Kasturi, S.P., et al., *Programming the magnitude and persistence of antibody responses with*
632 *innate immunity.* *Nature*, 2011. **470**(7335): p. 543-7.
- 633 13. Thanh Le, T., et al., *The COVID-19 vaccine development landscape.* *Nat Rev Drug Discov*,
634 2020. **19**(5): p. 305-306.
- 635 14. Jackson, N.A.C., et al., *The promise of mRNA vaccines: a biotech and industrial perspective.*
636 *NPJ Vaccines*, 2020. **5**: p. 11.
- 637 15. Hassett, K.J., et al., *Optimization of Lipid Nanoparticles for Intramuscular Administration of*
638 *mRNA Vaccines.* *Mol Ther Nucleic Acids*, 2019. **15**: p. 1-11.
- 639 16. Zeng, C., et al., *Formulation and Delivery Technologies for mRNA Vaccines.* *Curr Top*
640 *Microbiol Immunol*, 2020.
- 641 17. Fuller, D.H. and P. Berglund, *Amplifying RNA Vaccine Development.* *N Engl J Med*, 2020.
642 **382**(25): p. 2469-2471.
- 643 18. Chan, K.R., et al., *Cross-reactive antibodies enhance live attenuated virus infection for*
644 *increased immunogenicity.* *Nat Microbiol*, 2016. **1**: p. 16164.
- 645 19. Chan, C.Y., et al., *Early molecular correlates of adverse events following yellow fever*
646 *vaccination.* *JCI Insight*, 2017. **2**(19).
- 647 20. Chan, K.R., et al., *Metabolic perturbations and cellular stress underpin susceptibility to*
648 *symptomatic live-attenuated yellow fever infection.* *Nat Med*, 2019. **25**(8): p. 1218-1224.
- 649 21. Salti, S.M., et al., *Granzyme B regulates antiviral CD8+ T cell responses.* *J Immunol*, 2011.
650 **187**(12): p. 6301-9.
- 651 22. Ehrchen, J.M., et al., *The endogenous Toll-like receptor 4 agonist S100A8/S100A9*
652 *(calprotectin) as innate amplifier of infection, autoimmunity, and cancer.* *J Leukoc Biol*,
653 2009. **86**(3): p. 557-66.
- 654 23. Yu, G., et al., *APRIL and TALL-1 and receptors BCMA and TACI: system for regulating*
655 *humoral immunity.* *Nat Immunol*, 2000. **1**(3): p. 252-6.
- 656 24. Groom, J.R. and A.D. Luster, *CXCR3 in T cell function.* *Exp Cell Res*, 2011. **317**(5): p. 620-
657 31.
- 658 25. Conticello, S.G., et al., *Interaction between antibody-diversification enzyme AID and*
659 *spliceosome-associated factor CTNNB1.* *Mol Cell*, 2008. **31**(4): p. 474-84.
- 660 26. Premkumar, L., et al., *The receptor binding domain of the viral spike protein is an*
661 *immunodominant and highly specific target of antibodies in SARS-CoV-2 patients.* *Sci*
662 *Immunol*, 2020. **5**(48).
- 663 27. Rogers, T.F., et al., *Isolation of potent SARS-CoV-2 neutralizing antibodies and protection*
664 *from disease in a small animal model.* *Science*, 2020.
- 665 28. de Alwis, R., et al., *Impact of immune enhancement on Covid-19 polyclonal hyperimmune*
666 *globulin therapy and vaccine development.* *EBioMedicine*, 2020. **55**: p. 102768.
- 667 29. Honda-Okubo, Y., et al., *Severe acute respiratory syndrome-associated coronavirus vaccines*
668 *formulated with delta inulin adjuvants provide enhanced protection while ameliorating lung*
669 *eosinophilic immunopathology.* *J Virol*, 2015. **89**(6): p. 2995-3007.
- 670 30. Hashem, A.M., et al., *A Highly Immunogenic, Protective, and Safe Adenovirus-Based*
671 *Vaccine Expressing Middle East Respiratory Syndrome Coronavirus SI-CD40L Fusion*

- 672 *Protein in a Transgenic Human Dipeptidyl Peptidase 4 Mouse Model*. J Infect Dis, 2019.
673 **220**(10): p. 1558-1567.
- 674 31. Higgins, B.W., L.J. McHeyzer-Williams, and M.G. McHeyzer-Williams, *Programming*
675 *Isotype-Specific Plasma Cell Function*. Trends Immunol, 2019. **40**(4): p. 345-357.
- 676 32. Wec, A.Z., et al., *Longitudinal dynamics of the human B cell response to the yellow fever 17D*
677 *vaccine*. Proc Natl Acad Sci U S A, 2020. **117**(12): p. 6675-6685.
- 678 33. Tam, H.H., et al., *Sustained antigen availability during germinal center initiation enhances*
679 *antibody responses to vaccination*. Proc Natl Acad Sci U S A, 2016. **113**(43): p. E6639-
680 E6648.
- 681 34. Cirelli, K.M., et al., *Slow Delivery Immunization Enhances HIV Neutralizing Antibody and*
682 *Germinal Center Responses via Modulation of Immunodominance*. Cell, 2019. **177**(5): p.
683 1153-1171 e28.
- 684 35. von Herrath, M.G. and A. Bot, *Immune responsiveness, tolerance and dsRNA: implications*
685 *for traditional paradigms*. Trends Immunol, 2003. **24**(6): p. 289-93.
- 686 36. Jin, B., et al., *Immunomodulatory effects of dsRNA and its potential as vaccine adjuvant*. J
687 Biomed Biotechnol, 2010. **2010**: p. 690438.
- 688 37. Pepini, T., et al., *Induction of an IFN-Mediated Antiviral Response by a Self-Amplifying RNA*
689 *Vaccine: Implications for Vaccine Design*. J Immunol, 2017. **198**(10): p. 4012-4024.
- 690 38. Grifoni, A., et al., *Targets of T Cell Responses to SARS-CoV-2 Coronavirus in Humans with*
691 *COVID-19 Disease and Unexposed Individuals*. Cell, 2020. **181**(7): p. 1489-1501.e15.
- 692 39. Mateus, J., et al., *Selective and cross-reactive SARS-CoV-2 T cell epitopes in unexposed*
693 *humans*. Science, 2020.
- 694 40. Le Bert, N., et al., *SARS-CoV-2-specific T cell immunity in cases of COVID-19 and SARS,*
695 *and uninfected controls*. Nature, 2020.
- 696 41. Maruggi, G., et al., *Engineered alphavirus replicon vaccines based on known attenuated viral*
697 *mutants show limited effects on immunogenicity*. Virology, 2013. **447**(1-2): p. 254-64.
- 698 42. Thompson, J.M., et al., *Mucosal and systemic adjuvant activity of alphavirus replicon*
699 *particles*. Proc Natl Acad Sci U S A, 2006. **103**(10): p. 3722-7.
- 700 43. Ramaswamy, S., et al., *Systemic delivery of factor IX messenger RNA for protein replacement*
701 *therapy*. Proc Natl Acad Sci U S A, 2017. **114**(10): p. E1941-E1950.
- 702 44. Gan, E.S., et al., *Dengue virus induces PCSK9 expression to alter antiviral responses and*
703 *disease outcomes*. J Clin Invest, 2020.
- 704 45. Ayoub, A., et al., *Multiplex detection and dynamics of IgG antibodies to SARS-CoV2 and the*
705 *highly pathogenic human coronaviruses SARS-CoV and MERS-CoV*. J Clin Virol, 2020. **129**:
706 p. 104521.
- 707 46. Atyeo, C., et al., *Distinct early serological signatures track with SARS-CoV-2 survival*.
708 Immunity, 2020. **In Press**.
- 709 47. Tan, C.W., et al., *A SARS-CoV-2 surrogate virus neutralization test based on antibody-*
710 *mediated blockage of ACE2-spike protein-protein interaction*. Nat Biotechnol, 2020.
- 711 48. GeurtsvanKessel, C.H., et al., *An evaluation of COVID-19 serological assays informs future*
712 *diagnostics and exposure assessment*. Nat Commun, 2020. **11**(1): p. 3436.
- 713
- 714

715

FIGURES



716

717

718

719

720

721

722

723

724

725

726

727

728

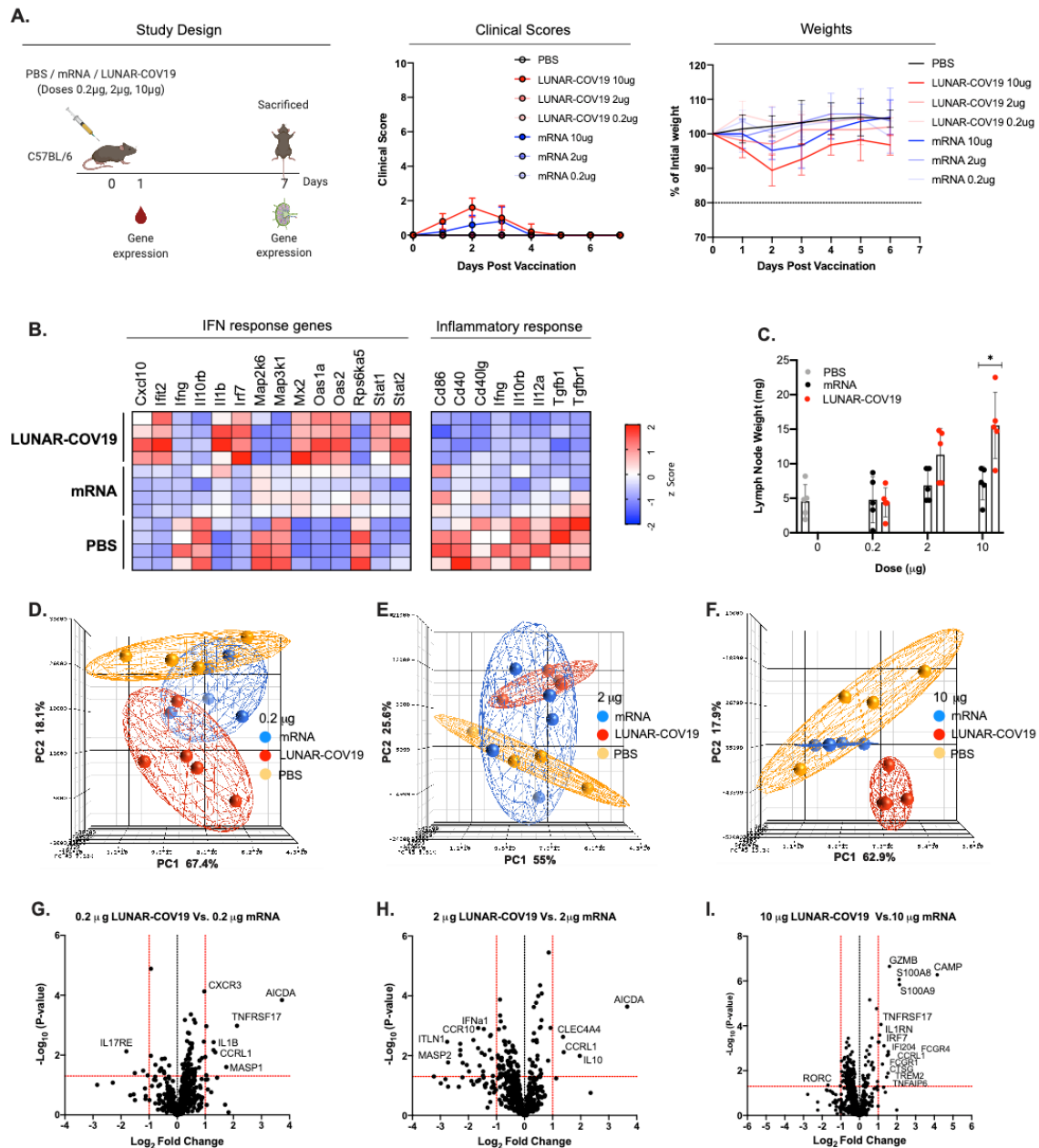
729

730

731

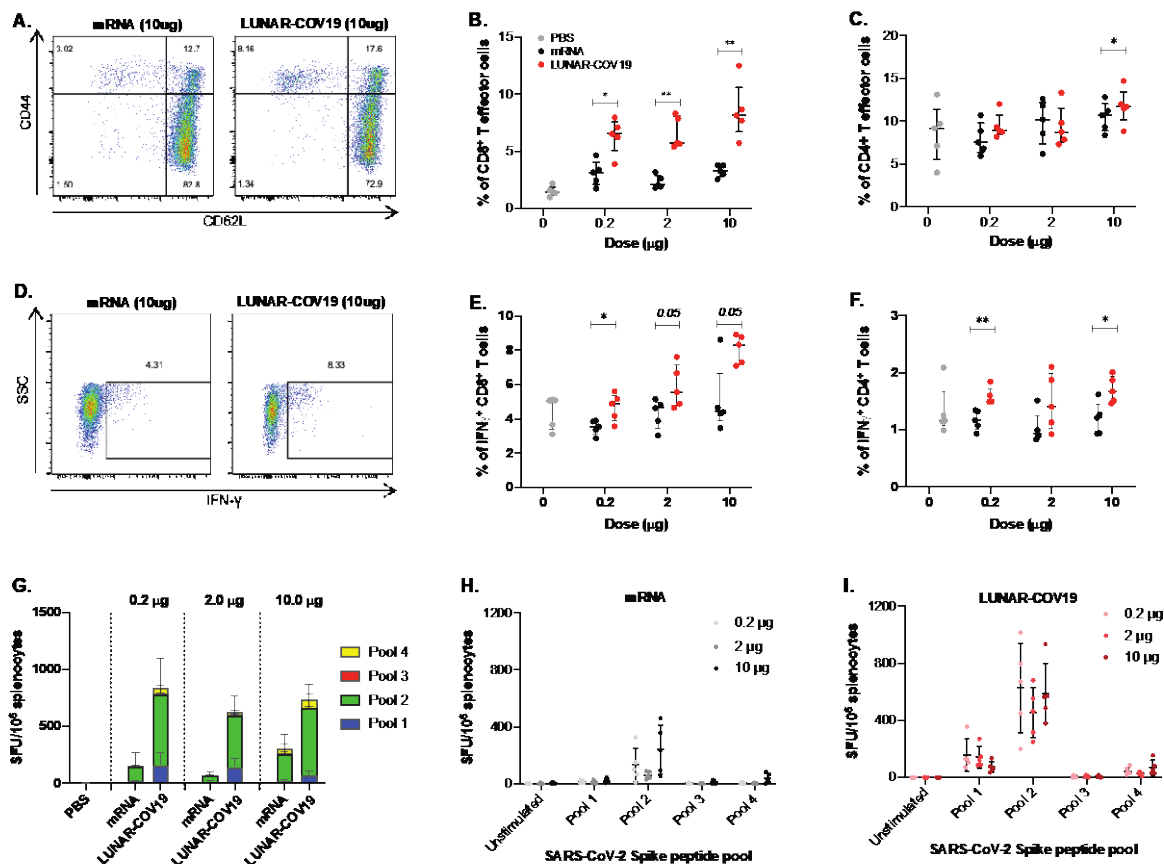
732

Figure 1. Design and Expression of a SARS-COV-2 vaccine with conventional mRNA and self-transcribing and replicating RNA (STARR[®]) platforms. **A)** Schematic diagram of the SARS-CoV-2 self-replicating STARR RNA (LUNAR[®]-COV19) and conventional mRNA vaccine constructs. The STARR construct encodes for the four non-structural proteins, ns1-ns4, from Venezuelan equine encephalitis virus (VEEV) and the unmodified full-length pre-fusion spike (S) protein of SARS-CoV-2. The mRNA construct also codes for the same SARS-CoV-2 full length spike S protein. **B)** Physical characteristics and RNA trapping efficiency of the LNP encapsulating conventional mRNA and LUNAR-COV19 vaccines. **C)** Western blot detection of SARS-CoV-2 S protein following transfection of HEK293 cells with LUNAR-COV19 and conventional mRNA. **D)** *In vivo* comparison of protein expression following IM administration of LNP containing luciferase-expressing STARR RNA or conventional mRNA. Balb/c mice ($n=3$ /group) were injected IM with 0.2 μ g, 2.0 μ g and 10.0 μ g of STARR RNA or conventional mRNA formulated with the same lipid nanoparticle. Luciferase expression was measured by *in vivo* bioluminescence on days 1, 3 and 7 post-IM administration. S domain 1 = S1, S domain 2 = S2, transmembrane domain = TM, cytoplasmic domain = CP; aka = also known as.



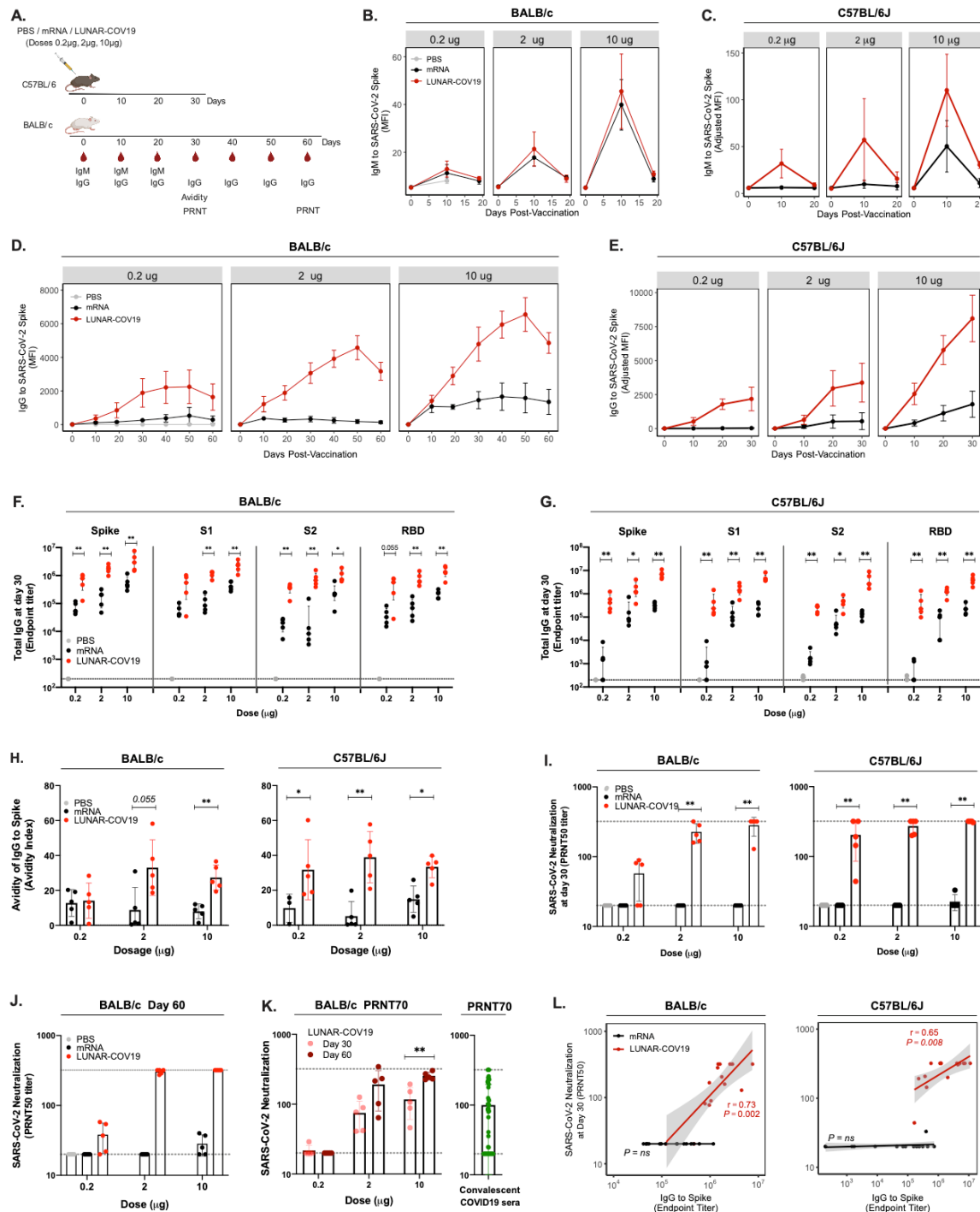
733
 734 **Figure 2: Clinical Scores, mouse weights and transcriptomic analysis of immune genes**
 735 **following vaccination with LUNAR-COV19 or conventional mRNA SARS-CoV-2**
 736 **vaccine candidates. A)** C57BL/6 mice ($n=5/\text{group}$) were immunized with either PBS,
 737 mRNA or LUNAR-COV19 (doses 0.2 µg, 2 µg or 10 µg), weight and clinical scores
 738 assessed every day, bled at day 1 post-immunization, sacrificed at 7 days post-vaccination
 739 and lymph nodes harvested. Gene expression of inflammatory genes and immune genes were
 740 measured in whole blood (at day 1) and lymph nodes (at day 7), respectively. **B)** Expression
 741 of IFN and inflammatory response genes in whole blood presented as heatmap of z scores. **C)**
 742 Lymph node weights at 7 days post-vaccination. Principal component analysis (PCA) of
 743 immune gene expression following vaccination with conventional mRNA or LUNAR-
 744 COV19 at doses **D)** 0.2 µg, **E)** 2 µg and **F)** 10 µg. Volcano plots of fold change of LUNAR-
 745 COV19 versus conventional mRNA (x-axis) and $\text{Log}_{10} P\text{-value}$ of LUNAR-COV19 versus
 746 conventional mRNA (y-axis) for doses **G)** 0.2 µg, **H)** 2 µg and **I)** 10 µg. Study design

747 schematic diagram created with BioRender.com. Weights of lymph nodes were compared
 748 between groups using a two-tailed Mann-Whitney *U* test with * denoting $0.05 < P < 0.01$.



749
 750
 751 **Figure 3. Cellular immune responses following vaccination with LUNAR-COV19 and**
 752 **conventional mRNA.** C57BL/6 mice ($n=5$ per group) were immunized with 0.2 μg, 2.0 μg,
 753 or 10.0 μg of LUNAR-COV19 or conventional mRNA via IM, sacrificed at day 7 post-
 754 vaccination and spleens analyzed for cellular T cell responses by flow-cytometry and
 755 ELISPOT. **A-B)** CD8⁺ and **C)** CD4⁺ T effector cells were assessed in vaccinated animals
 756 using surface staining for T cell markers and flow-cytometry. **D-E)** IFN γ ⁺ CD8⁺ T cells and
 757 **F)** Ratio of IFN γ ⁺/ IL4⁺ CD4⁺ T cells in spleens of immunized mice were assessed following
 758 *ex vivo* stimulation with PMA/IO and intracellular staining. **G-I)** SARS-CoV-2 S protein-
 759 specific responses to pooled S protein peptides were assessed using IFN γ ELISPOT assays
 760 following vaccination with mRNA (**H)** or LUNAR-COV19 (**I**). Percentage of CD8⁺ cells,
 761 CD4⁺ cells, IFN γ and IL4 producing T cells were compared between groups using two-tailed
 762 Mann-Whitney *U* test with * denoting $0.05 < P < 0.01$, and ** $0.01 < P < 0.001$.

763
 764
 765
 766
 767



768
769

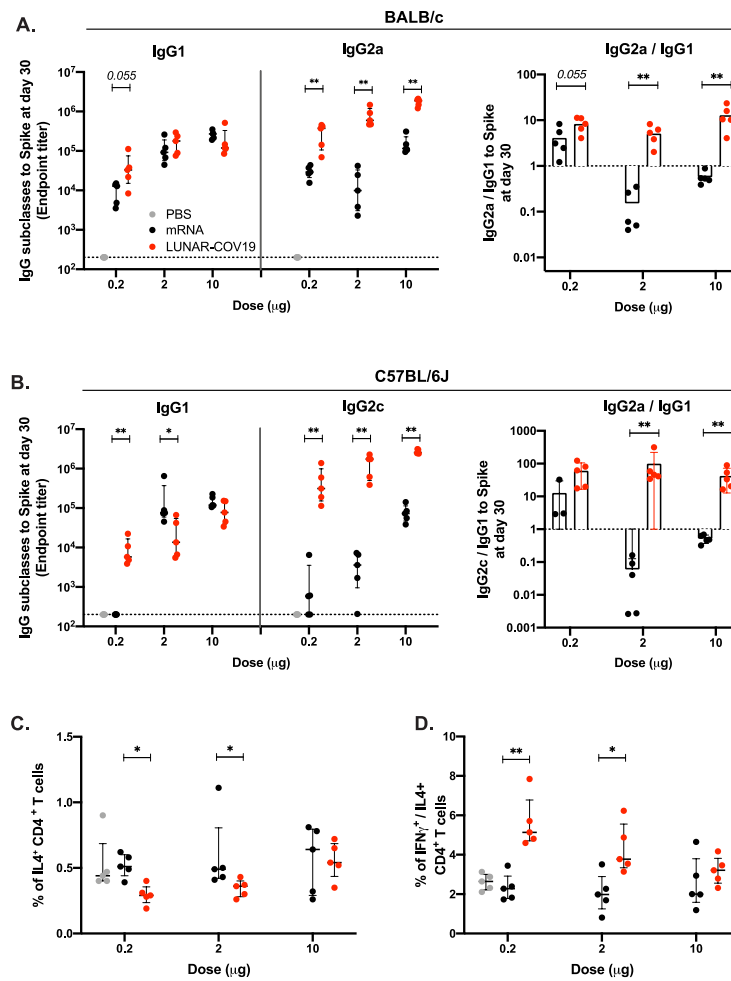
770 **Figure 4: LUNAR-COV19 elicits a higher quality humoral response than conventional**
 771 **mRNA platform.** A) BALB/c and C57BL/6J mice were immunized via IM with 0.2 µg, 2
 772 µg, or 10 µg of LUNAR-COV19 or conventional mRNA ($n=5$ /group). Blood sampling was
 773 conducted at baseline, and days 10, 19, 30, 40, 50 and 60 post-vaccination for BALB/c and
 774 days 10, 20 and 30 for C57BL/6J. B-C) IgM and D-E) IgG against the SARS-CoV-2 S
 775 protein over time, assessed using insect cell-derived whole S protein in a Luminex immuno-
 776 assay (measured as MFI). IgG endpoint titers to mammalian-derived whole S protein, S1, S2
 777 and RBD proteins to mammalian-derived whole S protein at day 30 post-vaccination were
 778 assessed in F) BALB/c and G) C57BL/6J. H) Avidity of SARS-CoV-2 S protein-specific

779 IgG at day 30 post-immunization was measured using 8M urea washes. **I)** Neutralizing
780 antibody (PRNT50 titers) at day 30 post-vaccination against a clinically isolated live SARS-
781 CoV-2 virus measured in both BALB/c and C57BL/6J. Gray dashed lines depict the serum
782 dilution range (i.e. from 1:20 to 1:320) tested by PRNT. **J)** PRNT50 and **K)** PRNT70 of
783 SARS-CoV-2 neutralization at day 30 and day 60 post-vaccination in BALB/c and
784 convalescent sera from COVID-19 patients. **L)** Correlation analysis of Spike-specific IgG
785 endpoint titers against SARS-CoV-2 neutralization (PRNT50). Antibody data were compared
786 between groups using a two-tailed Mann-Whitney *U* test with * denoting $0.05 < P < 0.01$, and
787 $**0.01 < P < 0.001$.

788

789

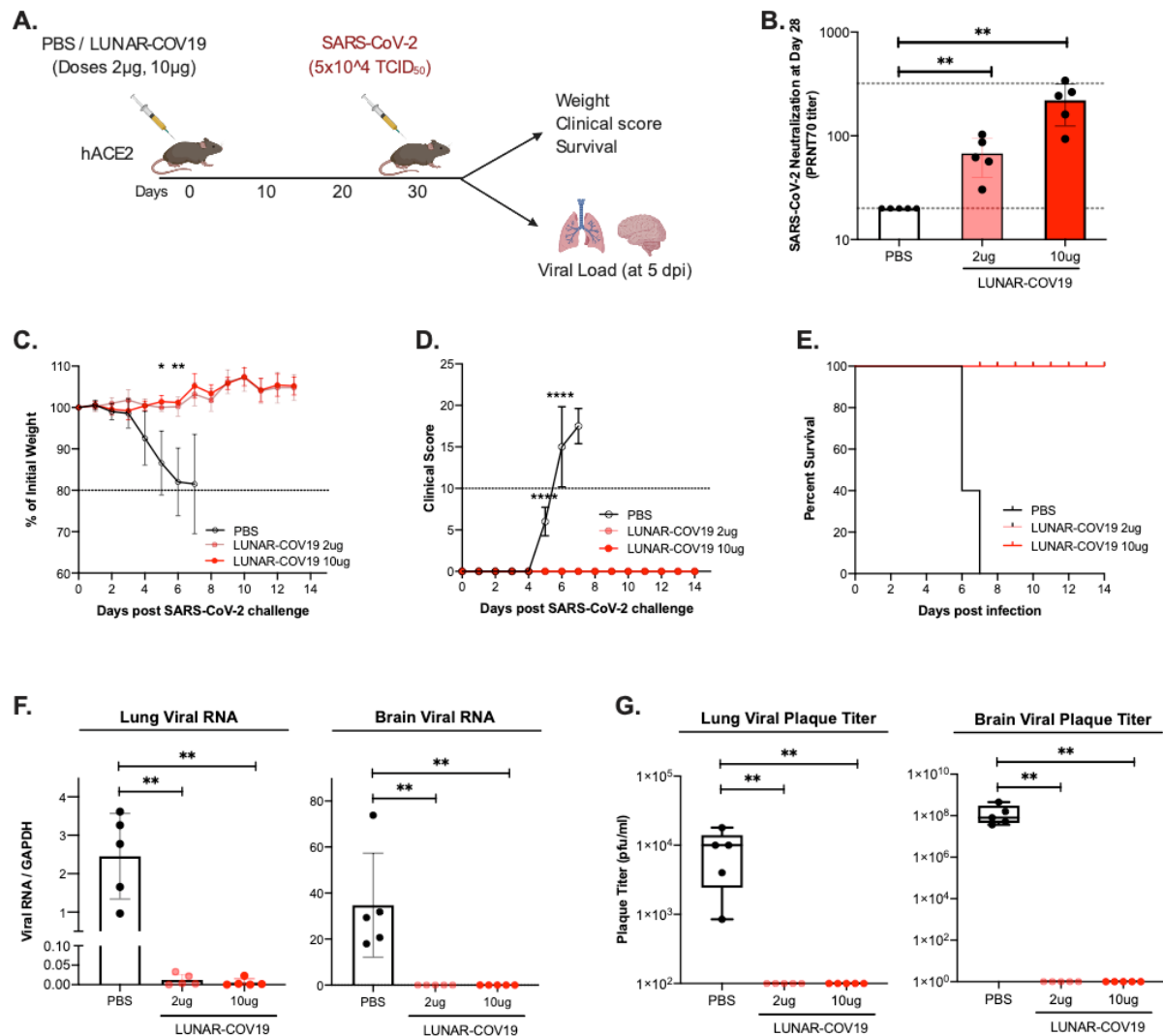
790



791
792

793 **Figure 5. LUNAR-COV19 elicits Th1 biased immune responses.** SARS-CoV-2 spike-
794 specific IgG subclasses and the ratio of IgG2a_c/IgG1 at 30 days post-vaccination with
795 LUNAR-COV19 and conventional mRNA in **A)** BALB/c and **B)** C57BL/6J mice. Th2
796 cytokine and Th1/Th2 skew in CD4 T cells at day 7 post-vaccination in C57BL/6J mice
797 measured by ICS as **C)** percentage of IL4⁺ CD4⁺ T cells and **D)** ratio of IFN γ ⁺/IL4⁺ CD4⁺ T
798 cells. Antibody titers and T cell data were compared between groups using a two-tailed
799 Mann-Whitney *U* test with * denoting 0.05 < *P* < 0.01, and ** 0.01 < *P* < 0.001.

800
801
802
803
804
805

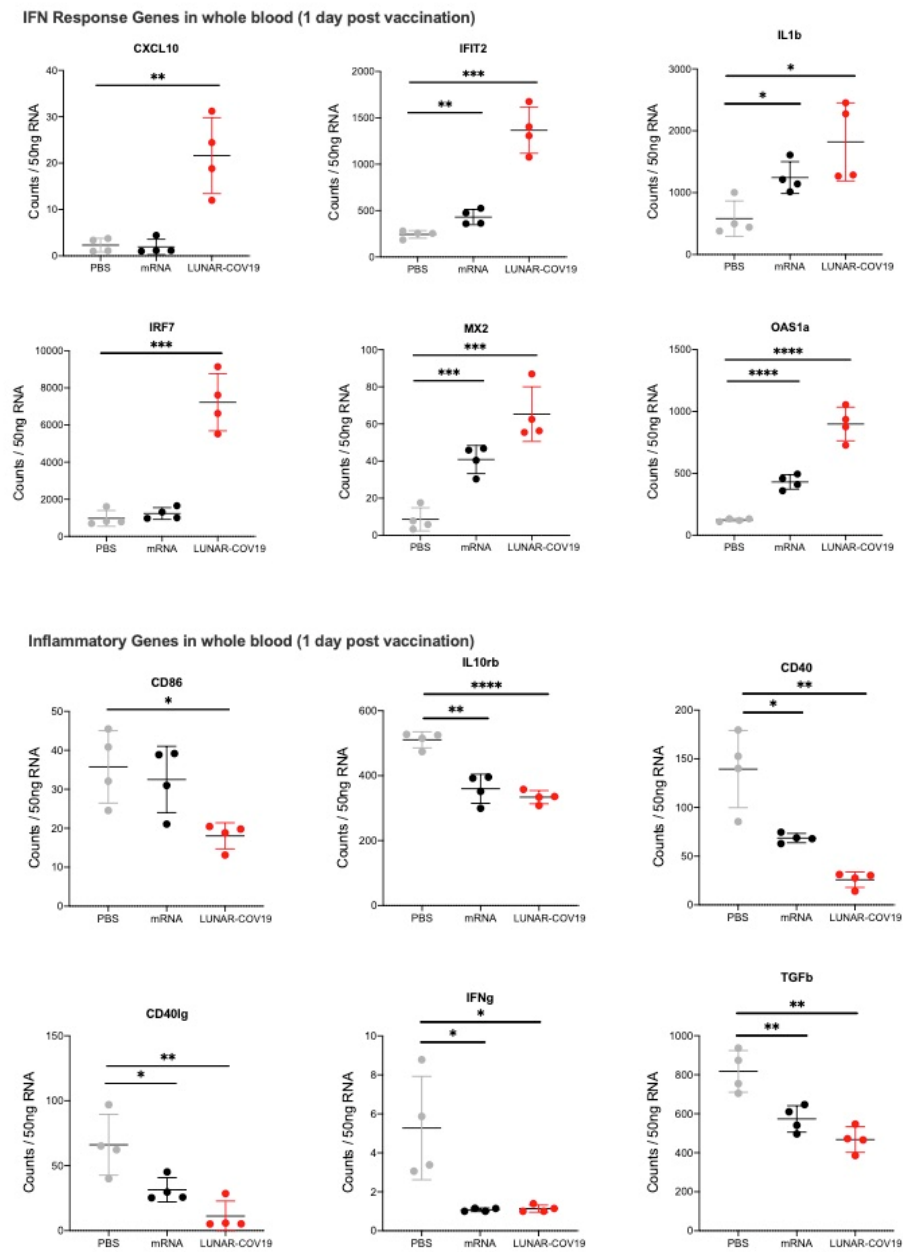


806
807

808 **Figure 6. Single dose of LUNAR-COV19 protects hACE2 mice against a lethal challenge**
 809 **of SARS-CoV-2 virus.** A) hACE2 transgenic mice were immunized with a single dose of
 810 either PBS or 2 µg or 10 µg of LUNAR-COV19 ($n=5$ per group), then challenged with live
 811 SARS-CoV-2 at 30 days post-vaccination, and assessed for either survival (with daily
 812 weights and clinical scores) or sacrificed at day 5 post-challenge and measured lung and
 813 brain tissue viral loads. Study design schematic diagram was created with BioRender.com B)
 814 Live SARS-CoV-2 neutralizing antibody titers (PRNT70) measured at 28 days post-
 815 vaccination. C) Weight, D) clinical score and E) survival was estimated following challenge
 816 with a lethal dose (5×10^5 TCID₅₀) of live SARS-CoV-2 virus. F) Viral RNA and G)
 817 infectious virus in the lungs and brain of challenged mice were measured with qRT-PCR or
 818 plaque assay, respectively. PRNT70 and viral titers (RNA and plaque titers) were compared
 819 across groups using the non-parametric Mann-Whitney U test. Weights and clinical scores at
 820 different timepoints were compared between PBS and 10µg LUNAR-CoV19 immunized
 821 mice using multiple t -tests. P -values are denoted by * for $0.05 < P < 0.01$, ** for $0.01 < P < 0.001$,
 822 *** for $0.001 < P < 0.0001$, **** $P < 0.00001$.

823
824

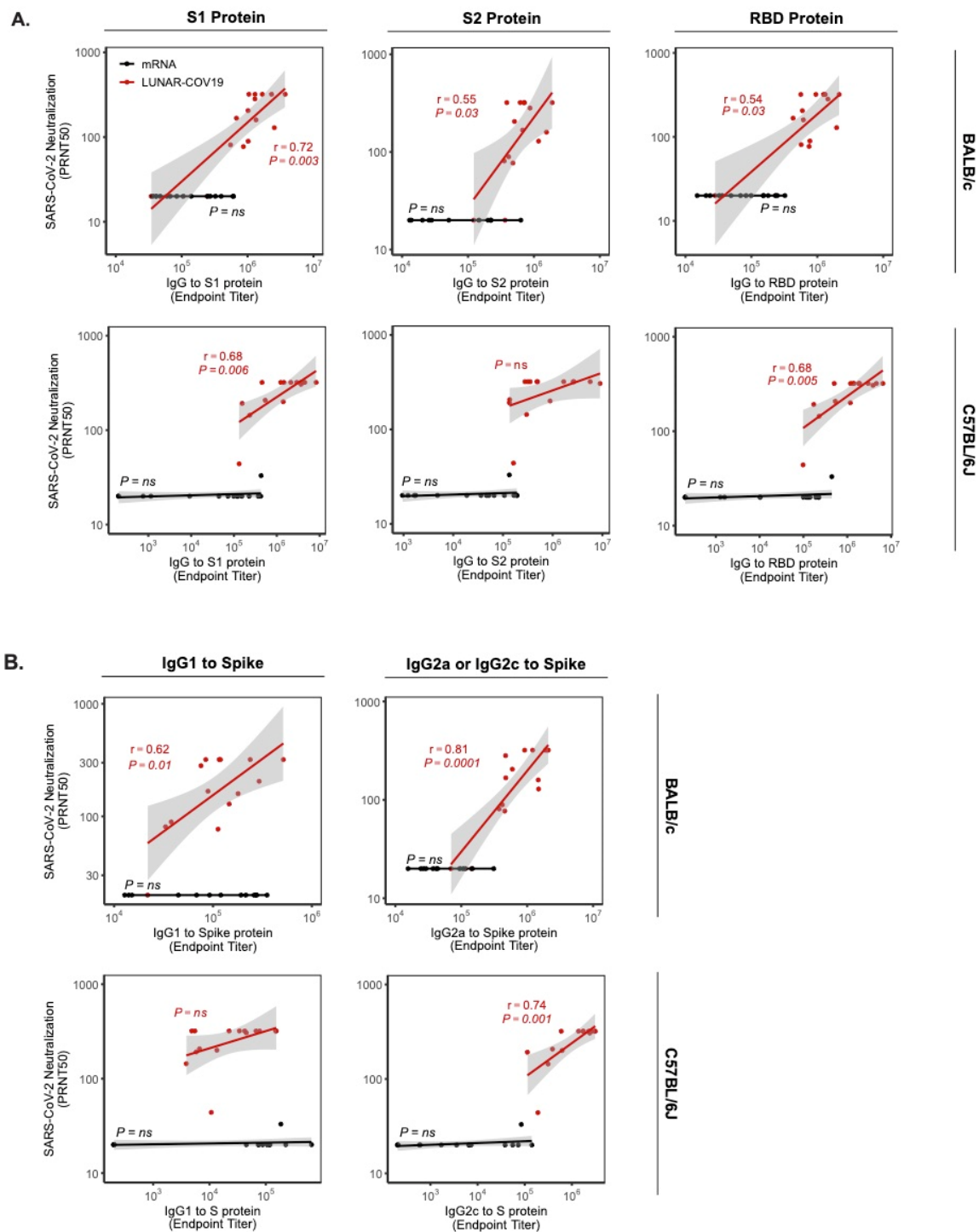
825
826



827
828
829
830
831
832
833

Supplementary Figure 1. Whole blood transcriptomic data at 1-day post-prime vaccination showing Nanostring counts per 50ng RNA of selected IFN and inflammatory genes.

834



835

836

837

838

839

840

841

842

Supplementary Figure 2. Correlation analysis of live SARS-CoV-2 neutralization against binding IgG and IgG subclasses in BALB/c and C57BL/6J mouse strains. **A)** Spearman correlation analysis of SARS-CoV-2 neutralization (PRNT50) against total IgG specific to several SARS-CoV2 antigens, including S, S1, and RBD recombinant proteins. **B)** Spearman correlation analysis of SARS-CoV-2 neutralization (PRNT50) against SARS-CoV2 S-specific IgG subclasses (IgG1 and IgG2a or IgG2c).